Cellular and Molecular Biology

Dong and Yang *Cell. Mol. Biol.*2016, 62 (12): 79-83
ISSN: 1165-158X
doi: 10.14715/cmb/2016.62.12.14

Original Research

Inhibition of matrix metalloproteins 9 attenuated *Candida albicans* induced inflammation in mouse cornea

C. Dong*, M. G. Yang

College of Biological Engineering, Henan University of Technology, Zhengzhou, Henan, China

Abstract: Since the severe corneal ulceration of mouse cornea is known to occur with inflammation. As one of imperative matrix metalloproteinase, the potential roles of matrix metalloproteins 9 (MMP9) in corneal ulceration and keratitis are still unveiled caused by fungal invasion. In this study, *Candida albicans (CA)* inoculated wild-type KM mice cornea was used as a model pathogen in corneal inflammation. *CA* invasion significantly stimulated the expression of collagen IV and MMP9 detected by RT-PCR, Real-time PCR and Immunofluorescent staining in mouse cornea as soon as 6 hours post infection, and relatively decreased at 1 day post infection. For examining the role of MMP9 in fungal keratitis, the mice corneas were subconjunctivally injected MMP9 antibody or recombinant MMP9 protein 6 hours prior to *CA* inoculation, using rabbit IgG as control. Subconjunctival injection of recombinant MMP9 protein prior to *CA* inoculation enhanced, whereas MMP9 antibody attenuated corneal ulceration and inflammation, examining basement membrane, fungal load, myeloperoxidase (MPO) and proinflammatory cytokines including Macrophage inflammatory protein 2 (MIP2), Interleukin-1β (IL-1β) and Tumor necrosis factor-α (TNF-α). Inhibition of MMP9 could potentially attenuate *Candida albicans* induced inflammation in mouse cornea.

Key words: Matrix metalloproteins 9, infection, inflammation.

Introduction

Serious infection caused by fungi is significantly increased in human (1). *Candida albicans* (*CA*) is the main cause of fungal infection leading to candidiasis (2), following with injury, surgery and contact lens wear. *CA*-keratitis is characterized by severe corneal ulceration caused by dissolution of the extracellular matrix (ECM) components of the cornea, leading to serious corneal scarring and perforation. Basement membrane is one thin layers of specialized ECM for supporting the growth of corneal epithelium cells. Modification of basement membrane proteins is imperative for tissue and ECM. The basement membrane proteins and oral mucosa protect the body from physical or chemical damage, heat, dehydration as well as infection (3).

Matrix metalloproteinases (MMPs) are family of Zn^{2+} and Ca^{2+} dependent proteolytic enzymes, involving in tissue remodeling and inflammation. MMPs have the broad activity to degrade all the components of ECM (4-6). In addition to their direct effects on ECM proteins, MMPs can induce the recruitment of inflammatory cells after infection by stimulating cytokines or generating chemotactic fragments from ECM protein. MMPs are grouped according to their structure and substrate, including collagenases, gelatinases, stromelysins and matrilysins. Of the 23 MMPs, MMP9 known as gelatinase B shows particular activity as a therapeutic target, giving the evidence of indicating its participation in pathological process of chronic inflammation, tumorigenesis and metatasis (4, 5, 7).

Previous report demonstrated that MMP9 $^{-/-}$ mice exhibited decreased disease severity in preclinical models of colitis and rheumatoid arthritis, as well as displaying reduced tumor growth and metastases in cancer models (8). However, the roles of MMP9 in *CA*-keratitis are still unclear. This study was sought to indicate whether MMP9 contributed to *CA*-caused corneal ulceration, and whether MMP9 could be therapeutically targeted for preventing *CA*-keratitis. Briefly, MMP9 expression in *CA*-challenged mouse cornea was assessed by Real-time PCR and immunohistochemistry analysis. Additionally, mouse cornea was subconjunctival injected MMP9 antibody (anti-MMP9) or MMP9 recombinant protein (rMMP9) prior to *CA* invasion. Corneal damage was examined by immunohistochemistry analysis of collagen IV, and disease severity was assessed by corneal imaging, clinical score, fungal burden, neutrophil infiltration and proinflammatory cytokines. Our result demonstrated *CA*-induced MMP9 probably attributed to corneal inflammation through degradation of basement membrane.

Materials and Methods

Fungi preparation

CA strain SC5314 was provided and confirmed taxonomically by Professor Ruifang Li from Henan University of Technology in September 2014. A clinical isolate was cultured for 3 days at 25°C. Using a predetermined conversion factor of 1 OD=3×10^7 CFU/ml at optical density (OD) 600 nm, the signal colony was harvested and diluted in sterile PBS (pH=7.4) to yield 1×10^5 colony-forming units (CFU)/5µl. The activity of each preparation was examined to produce a reproducible inflammatory response in mice corneas.

Received June 28, 2016; **Accepted** October 21, 2016; **Published** October 31, 2016

*** Corresponding author:** C. Dong, College of Biological Engineering, Henan University of Technology, Zhengzhou, Henan, China 450051. Email: chen.dong@haut.edu.cn

Table 1. Primers sequences used for RT-PCR and Real-time PCR.

Genes	Primer	Sequence
BD2	Forward	GCTTCAGTCATGAGGATCCATTAC
	Reverse	GCTAGGGAGCACTTGTTTGCATTT
MIP2	Forward	GAACATCCAGAGCTTGAGT
	Reverse	CTTTTTGACCGCCCTTGAGA
Collagen IV	Forward	GACCTGAAATTCTGCCAT
	Reverse	CAACCATCCTCCAGGACT
MMP9	Forward	GATCCCCAGAGCGTCATTC
	Reverse	TCCACCATTTGTCTGAATTCC
β-actin	Forward	AAGCCGGCTTCGCGGGCGA
	Reverse	CCACCTTGTTCACCTCATTTTG

Animals

Wild-type KM mice (age, 8 week; female; weight, 20-22 g) were purchased from Animal Center, Zhengzhou University. Animals were carefully housed and maintained on a 12 h light/dark cycle and given *ad libitum* access to food and water. Animals were treated in compliance with the Association for Research in Vision and Ophthalmology statement on the use of animals at Henan University of Technology (the approval number: 2014–091201).

Infection protocol

Mice (n=5/group) were anesthetized with 2 % Pelltobarbitalum Natricum and placed beneath a stereoscopic microscope for needle scratching (four 1-mm incisions using a sterile 26-gauge needle). The corneas were inoculated with 5 µl suspension containing 1×10^5 CFU of *CA* strain SC5314 (9, 10), using PBS as control. Eyes were examined to monitor the disease progression with microscope equipped with a digital camera.

RNA isolation, RT-PCR and Real-time PCR

The mice were sacrificed at 6 hours post infection (hpi) and 1 day post infection (dpi) respectively, then the corneas were excised from the enucleated mice eyes, minced and homogenized in PBS immediately. Total RNA of mice corneas was isolated using RNAprep pure Kit (Tiangen) according to manufacturer instructions. The first-strand cDNA was generated with Oligo (dT) primer using M-MLV reverse transcriptase (Promega), and RT-PCR was performed to examine the mRNA level of Macrophage inflammatory protein 2 (MIP2), β-defensin2 (BD2), Interleukin-1β (IL-1β), Tumor necrosis factor-α (TNF-α), collagen IV and MMP9, using β-actin as the reference gene (Table. 1). Real-time PCR was performed with the power SYBR Green PCR Master Mix (TAKARA) according the method described (11, 12).

Immunofluorescent staining

The eyes were removed from sacrificed mice at 1 dpi, and embedded in OCT compound. The corneas were cut 6 um thick by cryostat sectioning and the sections were mounted to polylysine-coated glass slides, and fixed in 4 % paraformaldehyde for 10 min. Sections were blocked with 10 mM PBS containing 2 % BSA for 1 hour at room temperature, and incubated with primary antibody: rabbit anti-mouse MMP9 (BOSTER, 1:100) or rabbit anti-mouse collagen IV (BOSTER, 1:150) overnight at 4°C, using rabbit IgG as the control. Then the section was incubated with secondary antibody: FITC conjugated goat anti-rabbit IgG (BOSTER, 1:100) for one hour. At last, the slides were mounted with DAPI mounting media.

Subconjunctival injection of MMP9 antibody or recombinant protein (rMMP9)

Mice (n=5/group) were anesthetized with 2 % Pelltobarbitalum Natricum. The corneas (n=5/group) were subconjunctivally injected 5 ug anti-MMP9 (BOSTER) or 2 ug rMMP9 (BOSTER) 6 hours prior to *CA* inoculation as method (9 ,10), using rabbit IgG as control. Eyes were photographed at 1 dpi by a digital camera equipped with microscope.

Clinical score, fungal burden determine, myeloperoxidase measurement and ELISA

The fungal load, myeloperoxidase (MPO) measurement and ELISA determination of each mouse cornea were performed by methods (9, 10). Briefly, the mice were sacrificed at 1 dpi, then corneas were excised from the enucleated mice eyes, minced and homogenized in 100 µl PBS containing 1mM PMSF. The homogenates of corneas were separated into two parts, one for plate fungal counting, and the other for MPO measurements, MIP2, IL-1β and TNF-α ELISA (BOSTER).

Statistical analysis

An unpaired, two-tailed student's t-test was used to determine statistical significance for data from Real-time PCR, fungal count, MPO assay and ELISA. Dates were presented as the means±SD. Statistical differences were considered significant at $*p<0.05$ or $**p<0.01$.

Results

***CA* invasion augmented expression of collagen IV and MMP9 in mouse cornea**

The effect of *CA* invasion on the expression pattern of MIP2, BD2, collagen IV and MMP9 in mouse cornea was investigated at 6 hpi and 1dpi. *CA* invasion induced expression of corneal MIP2 and BD2 at 6 hpi and 1 dpi (Figure 1a). Both MMP9 and collagen IV constitutively expressed in normal cornea. Interestingly, there was a significantly increasing in MMP9 and collagen IV during *CA* infection at 6 hpi and 1 dpi. Consistent with RT-PCR result, Real-time PCR also indicated *CA* inoculation up-regulated expression of corneal MIP2 at 6 hpi

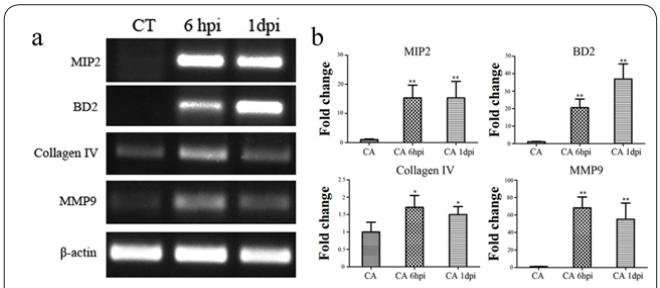

Figure 1. *CA* invasion elevated expression of corneal collagen IV and MMP9. Mice corneas were needle scratched and inoculated with 1×10^5 CFU of *CA,* using PBS treated cornea as control. Mice corneas were harvested at 6 hpi and 1 dpi respectively for examining expression profiling. RT-PCR (a) and Real-time PCR (b) were performed to examine the expression of MIP2, BD2, collagen IV and MMP9, using β-actin as the reference gene. Data of Real-time PCR was pooled from three independent experiments (n=3) and indicated *p* values were generated using unpaired student's *t*-test (**p*<0.05, ***p*<0.01).

(15.1) and 1 dpi (15.4), and augmented the level of BD2 at 6 hpi (20.3) and 1 dpi (37.1) using the normal cornea as control (Figure 1b). Additionally, MMP9 mRNA was increased as soon as 6 hpi (67.9 fold), then the mRNA level relatively down-regulated at 1 dpi (56.4 fold). At the same time, the mRNA level of collagen IV was increased at 6 hpi (1.72), and relatively decreased at 1 dpi (1.51).

Additionally, we tried to examine whether there was a parallel increasing in MMP9 protein levels by immunohistochemistry analysis. As shown in figure 2, the normal cornea had the basal level of MMP9, finding both in epithelial cells and stroma of corneas. *CA* invasion significantly augmented MMP9 expression throughout the corneal epithelium and stoma at 6 hpi, while it was decreased at 1 dpi.

CA-induced MMP9 resulted in degradation of basement membrane

To assess whether MMP9 resulted in corneal damage. Collagen IV was examined during MMP9 neutralization or rMMP9 injection, considering as the major component of basement membrane. As shown in figure 3, the normal cornea indicated the basal level of collagen IV between epithelial layer and stroma, staining

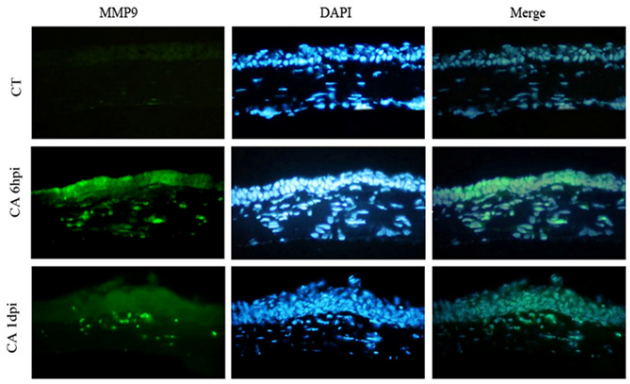

Figure 2. Immunostaining for MMP9 in *CA*-infected cornea vs normal cornea. Mice corneas in figure1 were embedded in OCT and sectioned. The sections were subjected to immunohistochemistry analysis with rabbit anti-mouse MMP9 antibody and DAPI staining for nuclei.

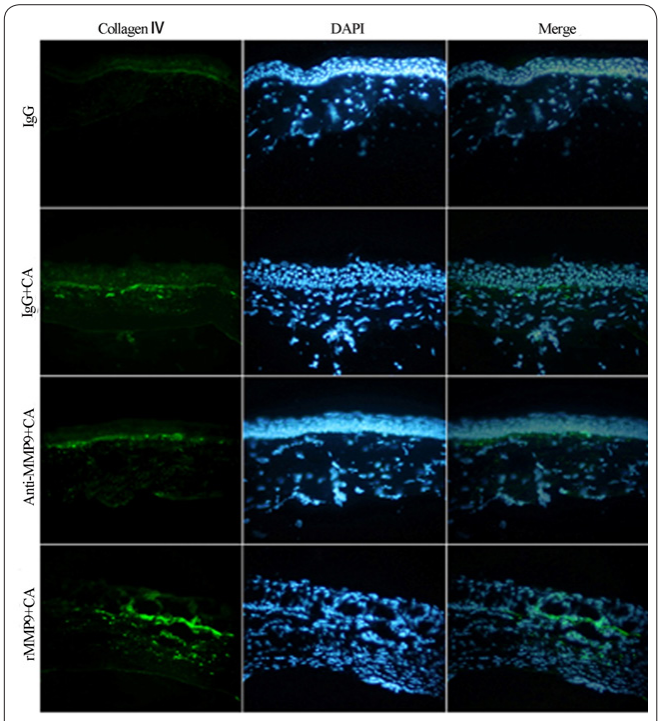

Figure 3. Effects of MMP9 on destruction of corneal basement membrane. Mice corneas were subconjunctivally injected anti-MMP9 or rMMP9 6 hours prior to *CA* inoculation, using rabbit IgG as the control. Mice corneas were embedded in OCT and sectioned at 1 dpi. The sections were subjected to immunohistochemistry analysis with rabbit anti-mouse collagen IV antibody and DAPI staining for nuclei.

for collagen IV was even and uninterrupted in intact cornea (IgG). *CA* inoculation significantly elevated the expression of collagen IV in cornea injected by IgG (IgG+CA), and partly disrupted the corneal basement membrane. Additionally, staining for collagen IV was more even and uninterrupted in the cornea anti-MMP9 injected (anti-MMP9+CA) compared to the infected cornea (IgG+CA) at 1 dpi, while it was almost completely interrupted in the cornea rMMP9 treated (rMMP9+CA).

MMP9 contributed to corneal inflammation caused by *CA* invasion

Having proved *CA* invasion resulted in corneal damage, we tried to demonstrate the role of MMP9 in corneal inflammation. The mice corneas were subconjunctival injected anti-MMP9 or rMMP9 6 hours prior to *CA* inoculation using IgG as control. Mice corneas were photographed, and disease severity was assayed by clinical score, fungal burden, polymorphonuclear neutrophil (PMN) infiltration and proinflammatory cytokines at 1 dpi. As shown in figure 4a, the control cornea (IgG+CA) pretreated with IgG was partially opaque. The opacity was greatly decreased in corneas injected with anti-MMP9 (anti-MMP9+CA), increasing in cornea treated with rMMP9 (rMMP9+CA) compared with control cornea. Clinical score indicated corneas injected with anti-MMP9 (anti-MMP9+CA) had significantly less *CA*-keratitis than the control cornea (Figure 4b), while severity of *CA*-keratitis was more serious in corneas injected with rMMP9 (rMMP9+CA). As shown in figure 4c, 2.5×10^3 CFU of *CA* were detected in the control cornea (IgG+CA), while inhibition of MMP9 (anti-MMP9+CA) resulted in significant decrease of fungal load (2.5 fold), and injection of rMMP9

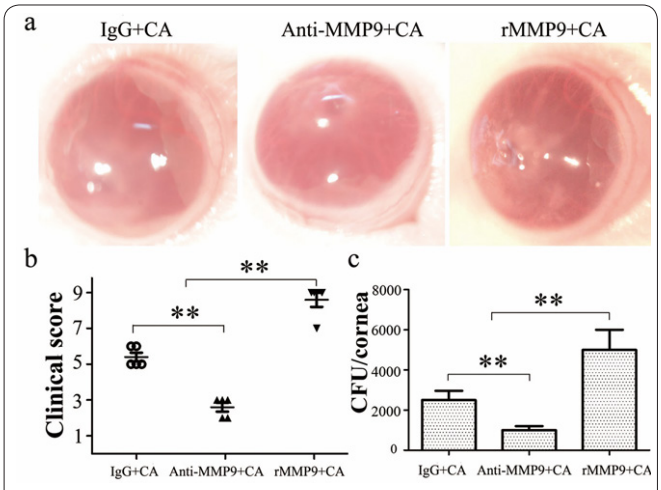

Figure 4. Role of MMP9 in *CA*-keratitis. Mice corneas were subconjunctivally injected anti-MMP9 or rMMP9 6 hours prior to *CA* inoculation, using rabbit IgG as the control. The corneas were photographed at 1 dpi (a), and homogenized for clinical score (b) and fungal burden (c). Data was pooled from five independent experiments (n=5) and indicated *p* values were generated using unpaired student's *t*-test (*p<0.05, **p<0.01).

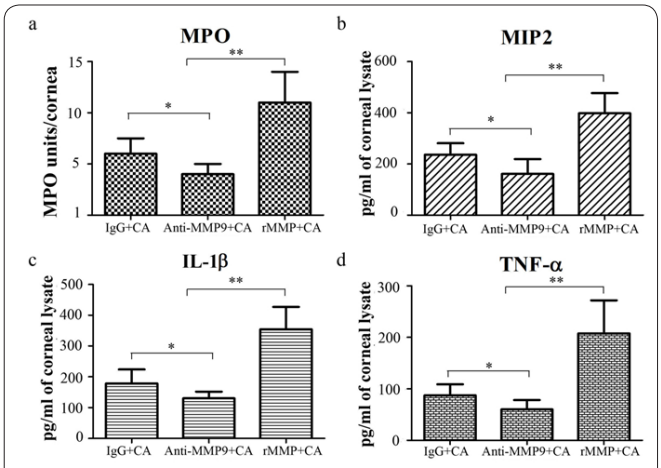

Figure 5. MPO assay and ELISA for MIP2, IL-1β and TNF-α. Mice corneas homogenized in figure 4 were examined for MPO activity (a), MIP2 (b), IL-1β (c) and TNF-α determination (d). Data was pooled from five independent experiments (n=5) and indicated *p* values were generated using unpaired student's *t*-test (*p<0.05, **p<0.01).

(rMMP9+CA) elevated fungal burden (2.1 fold). At the same time, PMN infiltration (Figure 5a) and levels of MIP2 (Figure 5b), IL-1β (Figure 5c) and TNF-α (Figure 5d) were significantly attenuated in anti-MMP9 treated cornea (anti-MMP9+CA), conversely all of them were up-regulated in rMMP9 injected cornea (rMMP9+CA).

Discussion

CA infection resulted in corneal damage, leading to the separation of epithelial cells and a reduction in thickness (13). Some physiological mechanisms such as expression and production of basement membrane protein also were activated. Using *CA*-infected mouse cornea as a model pathogen, our result demonstrated *CA* invasion stimulated the expression of MIP2 and BD2 (Figure 1). As the major component of basement membrane protein, collagen IV was constitutively expressed in the cornea of normal mice, and significantly elevated during *CA* infection (Figure 1). In addition to stimulate collagen IV, various agents such as pathogens and inflammatory cytokines had been implicated in the activation of MMPs, which were part of the cornea's response to infection (14). Among the MMPs, MMP9 had been considered as the most imperative enzyme in cleaving corneal basement membrane components (15-17). It was reported MMP9 was significantly up-regulated in liver diseases such as liver fibrosis and acute hepatitis, and inhibition of MMP9 prevented liver damage (18). Increased production of MMP9 by the corneal epithelium had been found in the eyes of individuals with sterile corneal ulceration (19). Corneal MMP9 increased as soon as 6 hpi, and relatively decreased at later infective period (Figure 1). Transcriptional up-regulation was parallel with an increase in the level of MMP9 protein expressed in corneal epithelium and stroma (Figure 2). Based on the results described above, it was concluded that *CA* invasion probably stimulated MMP9 to degrade corneal basement membrane, with the up-regulation of collagen IV in host cells in order to maintain tissue integrity.

In order to further assess the role of *CA*-induced MMP9 in destruction of corneal basement membrane, anti-MMP9 and rMMP9 were performed to demonstrate the contribution of MMP9 in corneal damage. As shown in figure 3, collagen IV were elevated by *CA* invasion. Immunostaining for collagen IV confirmed an interrupted basement membrane in the control cornea (IgG+CA) versus MMP9 inhibited cornea (anti-MMP9+CA), while basement membrane was more injured in the cornea rMMP9 injected (rMMP9+CA) than the control group (Figure 3). This results demonstrated that *CA*-induced MMP9 resulted in proteolysis of the basement membrane proteins, contributing to the loss of integrity of corneal epithelial barrier.

Additionally, it was reported disruption of epithelial basement membrane facilitated PMN transmigration to the site of inflammation in different corneal ulcerative models (20). The role of MMP9 in *CA*-keratitis was further confirmed during anti-MMP9 or rMMP9 injected. The cornea injected by rMMP9 (rMMP9+CA) exhibited more serious corneal disease and fungal load than control groups (IgG+CA), conversely cornea injected by anti-MMP9 (anti-MMP9+CA) showed less disease and fungal number (Figure 4). Moreover, inhibition of MMP9 significantly attenuated PMNs compared with control group, measuring by MPO activity (Figure 5a). Consistent with this result, PMNs were augmented in the rMMP9 injected cornea, proving that MMP9 contributed to the transmigration of PMNs into cornea. MMP9 could directly degrade stromal collagen and produce collagen peptide fragments that were chemotactic for PMNs (21). The inflammation, consisting mainly of PMNs, also was confirmed by MIP2, IL-1β and TNF-α in the cornea treated by anti-MMP9 (anti-MMP9+CA) or rMMP9 (rMMP9+CA) versus control cornea (Figure 5b, 5c and 5d).

Up to now, lots of pathologies associate with dysregulation of MMP9 in both human diseases and animal models of disease, supporting the trend that MMP9 is a therapeutic target (22-24). This study demonstrated MMP9 played an imperative role in inflammatory response through corneal ulceration. Degradation of

corneal basement membrane by MMP9 altered cell-matrix and enhanced cornea susceptibility to *CA* invasion. MMP9 activity in *CA*-keratitis was implicated in stimulation proinflammatory cytokines such as MIP2, IL-1β and TNF-α as well as regulation of PMN transmigration into the cornea. Depending on *CA* inoculated mouse cornea model, our data demonstrated that MMP9 contributed to *CA*-induced corneal inflammation. This finding provided a worthwhile therapeutics for combating corneal destruction and inflammation caused by fungal invasion.

Acknowledgments

The authors are greatly appreciative of Professor Huiru Zhang for their helpful comments and detailed suggestions. This work is financially supported by Doctoral Scientific Research Start-up Foundation from Henan University of Technology (no.31400855), and Fundamental Research Funds for the Henan Provincial Colleges and Universities in Henan University of Technology (no. 2015QNJH07).

References

1. Odom DC, Reno HE. Fungal infections in the hospitalized patient. Hosp Med Clinic 2015; 4: 313-327.
2. Calderone RA, Fonzi WA. Virulence factors of Candida albicans. Trends Microbiol 2001; 9: 327-335.
3. French KR, Pollitt CC. Equine laminitis: cleavage of laminin 5 associated with basement membrane dysadhesion. Equine Vet J 2004; 36: 242-247.
4. Roy R, Yang J, Moses MA. Matrix metalloproteinases as novel biomarkers and potential therapeutic targets in human cancer. J Clin Oncol 2009; 27(31): 5287-5297.
5. Vandooren J, Van den Steen PE, Opdenakker G. Biochemistry and molecular biology of gelatinase B or matrix metalloproteinase-9 (MMP-9): the next decade. Crit Rev Biochem Mol 2013; 48(3): 222 -272.
6. Page-McCaw A, Ewald AJ, Werb Z. Matrix metalloproteinases and the regulation of tissue remodel-ling. Nat Rev Mol Cell Bio 2007; 8(3): 221 - 233.
7. Van den Steen PE, Dubois B, Nelissen I, Rudd PM, Dwek RA, Opdenakker G. Biochemistry and molecular biology of gelatinase B or matrix metalloproteinase- 9 (MMP-9). Crit Rev Biochem Mol Biol 2002; 37: 375-536.
8. Martin MD, Carter KJ, Jean-Philippe SR, Chang M, Mobashery S, Thiolloy S. Effect of ablation or inhibition of stromal matrix metalloproteinase-9 on lung metastasis in a breast cancer model is de-pendent on genetic background. Cancer Res 2008; 68(15): 6251 -6259.
9. Yoon GS, Dong C, Gao N, Kumar A, Standiford TJ, Yu FS. Interferon regulatory factor-1 in flagellin-induced reprogramming: potential protective role of CXCL10 in cornea innate defense against Pseudomonas aeruginosa infection. Invest Ophthalmol Vis Sci 2013; 54(12): 7510-21.
10. Liu XW, Gao N, Dong C, Standiford TJ, Liu ZG, Yu FS. Flagellin-induced expression of CXCL10 mediates direct fungal killing and recruitment of NK cells to the cornea in response to Candida albicans infection. Eur J Immunol 2014; 44(9): 2667-79.
11. Dong C, Zheng XF, Li GL, Pan C, Zhou MQ, Hu ZL. Cloning and expression of one chloroplastic ascorbate peroxidase gene from Nelumbo nucifera. Biochem Genetics 2011a; 49(9): 656-664.
12. Dong C, Zheng XF, Li GL, Zhu HL, Zhou MQ, Hu ZL. Molecular cloning and expression of two cytosolic copper-zinc superoxide dismutases genes from Nelumbo nucifera. Appl Biochem Biotechnol 2011b; 163 (5): 679-691.
13. Mostefaoui Y, Claveau I, Rouabhia M. In vitro analyses of tissue structure and interleukin-1h expression and production by human oral mucosa in response to Candida albicans infections. Cytokine 2004; 25: 162 -171.
14. Wong TT, Sethi C, Daniels JT, Limb GA, Murphy G, Khaw PT. Matrix metalloproteinases in disease and repair processes in the anterior segment. Surv Ophthalmol 2002; 47: 239–256.
15. Asahi M, Wang X, Mori T, Sumii T, Jung JC, Moakowitz MA. Effects of matrix metalloprotein-ase-9 gene knock-out on the proteolysis of blood-brain barrier and white matter components after cerebral ischemia. J Neurosci 2001; 21: 7724 -7732.
16. Sternlicht M, Werb Z. How matrix metalloproteinases regulate cell behavior. Ann Rev Cell Dev Biol 2001; 17: 463–516.
17. Behzadian MA, Wang XL, Windsor LJ, Ghaly N, Caldwell RB. TGF-beta increases retinal endothelial cell permeability by increasing MMP-9: possible role of glial cells in endothelial barrier function. Invest Ophthalmol Vis Sci 2001; 42: 853– 859.
18. Wielockx B, Lannoy K, Shapiro SD, Itoh T, Itohara S, Vandekerckhove J. Inhibition of matrix metalloproteinases blocks lethal hepatitis and apoptosis induced by tumor necrosis factor and allows safe antitumor therapy. Nat Med 2001; **7**: 1202-1208.
19. De Paiva CS, Corrales RM, Villarreal AL, Farley WJ, Li DQ, Stern ME, Pflugfelder SC. Corticosteroid and doxycycline suppress MMP-9 and inflammatory cytokine expression, MAPK activation in the corneal epithelium in experimental dry eye. Exp Eye Res 2006; 83(3): 526-35.
20. Chin AC, Parkos CA. Pathobiology of neutrophil transepithelial migration: implication in mediating epithelial injury. Annu Rev Pathol 2007; 2: 111-43.
21. Adair-Kirk TL, Senior RM. Fragments of extracellular matrix as mediators of inflammation. Int J Biochem Cell Biol 2008; 40(6-7): 1101-10.
22. Devy L, Dransfield DT. New Strategies for the Next Generation of Matrix-Metalloproteinase Inhibitors: Selectively Targeting Membrane-Anchored MMPs with Therapeutic Antibodies. Biochem Res Int 2011; 2011: 191670.
23. Gialeli C, Theocharis AD, Karamanos NK. Roles of matrix metalloproteinases in cancer progression and their pharmacological targeting. FEBS J 2011; 278(1): 16 -27.
24. Wang X, Li KF, Adams E, Van Schepdael A. Matrix metalloproteinase inhibitors: a review on bioanaly-tical methods, pharmacokinetics and metabolism. Curr Drug Metab 2011; 12(4): 395 -410.